



Exclusive $pp \rightarrow ppK^{*0}\bar{K}^{*0}$ reaction: $f_2(1950)$ resonance versus diffractive continuum

Piotr Lebedowicz [Piotr.Lebedowicz@ifj.edu.pl]

Institute of Nuclear Physics Polish Academy of Sciences, Radzikowskiego 152, PL-31342 Kraków, Poland

EPS-HEP Conference 2021, European Physical Society conference on High Energy Physics, July 26–30, 2021, Online conference hosted jointly by Universität Hamburg and DESY, Germany

Abstract

We present first predictions of the cross sections and differential distributions for the exclusive reaction $pp \rightarrow pp(K^{*0}\bar{K}^{*0} \rightarrow K^+\pi^-K^-\pi^+)$ [1]. The amplitudes for the reaction are formulated within the tensor-pomeron approach [2, 3]. We consider separately the $f_2(1950)$ s-channel exchange mechanism and the reggeized- K^{*0} -exchange mechanism. First mechanism is a candidate for the central diffractive production of tensor glueball and the second one is an irreducible continuum. We adjust parameters of our model for the reaction $pp \rightarrow ppK^{*0}\bar{K}^{*0}$, assuming the dominance of pomeron-pomeron fusion, to the WA102 experimental data [4]. We find that including the continuum contribution alone one can describe the WA102 data reasonably well. We present predictions for the reaction $pp \rightarrow ppK^+K^-\pi^+\pi^-$ for the LHC experiments at $\sqrt{s} = 13$ TeV. We find cross sections $\sigma \simeq 17 - 250$ nb depending on the assumed cuts.

Formalism

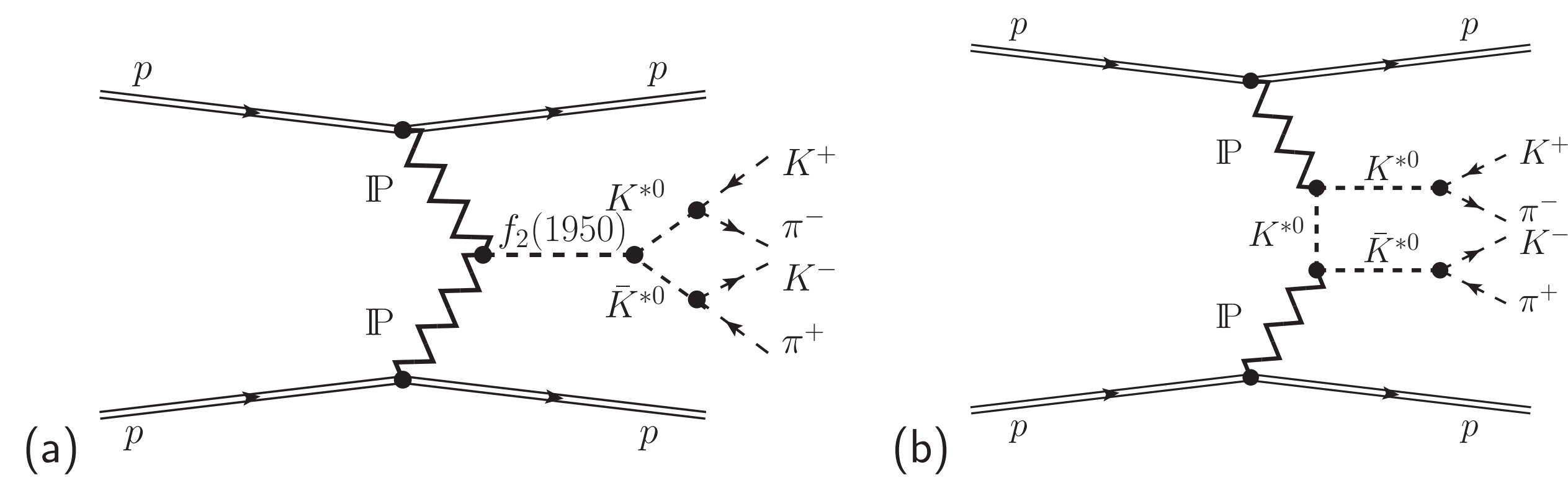


Fig.1: “Born-level” diagrams for double pomeron (IP) central exclusive production (CEP) of $K^{*0}\bar{K}^{*0}$ states and their subsequent decays into $K^+\pi^-K^-\pi^+$ in proton-proton collisions: (a) mechanism through the $f_2(1950)$, (b) continuum mechanism with reggeized K^* exchange.

We treat effectively the $2 \rightarrow 6$ process, as arising from the $pp \rightarrow ppK^{*0}\bar{K}^{*0}$ reaction (with f_{K^*} the spectral functions of K^{*0} mesons):

$$\sigma_{2 \rightarrow 6} = \int_{m_K + m_\pi}^{\max\{m_{X_3}\}} \int_{m_K + m_\pi}^{\max\{m_{X_4}\}} \sigma_{2 \rightarrow 4}(\dots, m_{X_3}, m_{X_4}) f_{K^*}(m_{X_3}) f_{K^*}(m_{X_4}) dm_{X_3} dm_{X_4}. \quad (1)$$

We include absorptive corrections to the Born amplitudes in the one-channel eikonal approximation; for more details see [1].

The Born-level amplitude for the $2 \rightarrow 4$ reaction $p(p_a, \lambda_a) + p(p_b, \lambda_b) \rightarrow p(p_1, \lambda_1) + p(p_2, \lambda_2) + K^{*0}(p_3, \lambda_3) + \bar{K}^{*0}(p_4, \lambda_4)$ via the $\text{IP} \text{IP} \rightarrow f_2(1950)$ fusion mechanism can be written as

$$\begin{aligned} \mathcal{M}_{\lambda_a \lambda_b \rightarrow \lambda_1 \lambda_2 \lambda_3 \lambda_4}^{(\text{IP} \text{IP} \rightarrow f_2 \rightarrow K^* \bar{K}^*)} &= (-i) \left(\epsilon_{\kappa_3}^{(K^*)}(\lambda_3) \right)^* \left(\epsilon_{\kappa_4}^{(\bar{K}^*)}(\lambda_4) \right)^* \bar{u}(p_1, \lambda_1) i\Gamma^{(\text{IP} \text{IP})} \mu_1 \nu_1(p_1, p_a) u(p_a, \lambda_a) i\Delta_{\mu_1 \nu_1, \alpha_1 \beta_1}^{(\text{IP})}(s_1, t_1) \\ &\times i\Gamma^{(\text{IP} \text{IP} f_2)} \alpha_1 \beta_1 \alpha_2 \beta_2 \rho \sigma(q_1, q_2) i\Delta_{\rho \sigma, \alpha \beta}^{(f_2)}(p_{34}) i\Gamma^{(f_2 K^* \bar{K}^*)} \alpha \beta \kappa_3 \kappa_4(p_3, p_4) \\ &\times i\Delta_{\alpha_2 \beta_2, \mu_2 \nu_2}^{(\text{IP})}(s_2, t_2) \bar{u}(p_2, \lambda_2) i\Gamma^{(\text{IP} \text{IP})} \mu_2 \nu_2(p_2, p_b) u(p_b, \lambda_b), \end{aligned} \quad (2)$$

where $s_1 = (p_1 + p_3 + p_4)^2$, $s_2 = (p_2 + p_3 + p_4)^2$, $q_1 = p_a - p_1$, $q_2 = p_b - p_2$, $t_1 = q_1^2$, $t_2 = q_2^2$, and $p_{34} = q_1 + q_2$. $\Gamma^{(\text{IP} \text{IP})}$ and $\Delta^{(\text{IP})}$ denote the effective proton vertex function and propagator, respectively, for the tensor-pomeron exchange (see [2]):

$$i\Gamma_{\mu\nu}^{(\text{IP} \text{IP})}(p', p) = -i3\beta_{\text{P}NN} F_1(t) \left\{ \frac{1}{2} [\gamma_\mu(p' + p)_\nu + \gamma_\nu(p' + p)_\mu] - \frac{1}{4} g_{\mu\nu}(\not{p}' + \not{p}) \right\}, \quad (3)$$

$$i\Delta_{\mu\nu, \kappa\lambda}^{(\text{IP})}(s, t) = \frac{1}{4s} \left(g_{\mu\kappa} g_{\nu\lambda} + g_{\mu\lambda} g_{\nu\kappa} - \frac{1}{2} g_{\mu\nu} g_{\kappa\lambda} \right) (-is\alpha'_P)^{\alpha_P(t)-1}, \quad (4)$$

where $\beta_{\text{P}NN} = 1.87 \text{ GeV}^{-1}$, $F_1(t)$ is the Dirac form factor of the proton, and $\alpha_P(t)$ the pomeron trajectory: $\alpha_P(t) = \alpha_P(0) + \alpha'_P t$, $\alpha_P(0) = 1.0808$, $\alpha'_P = 0.25 \text{ GeV}^{-2}$. A possible choice for the $i\Gamma_{\mu\nu, \kappa\lambda, \rho\sigma}^{(\text{IP} \text{IP} f_2)(j)}$ coupling terms $j = 1, \dots, 7$, derived from a corresponding coupling Lagrangians, is given in [3]. We assume, that only the $j = 1$ coupling, corresponding to the lowest values of orbital angular momentum and spin of the two “real pomerons” (J, S) = (0, 2), is unequal to zero. The $\text{IP} \text{IP} f_2$ vertex supplemented by form factors is

$$i\Gamma_{\mu\nu, \kappa\lambda, \rho\sigma}^{(\text{IP} \text{IP} f_2)}(q_1, q_2) = i\Gamma_{\mu\nu, \kappa\lambda, \rho\sigma}^{(\text{IP} \text{IP} f_2)(1)} \tilde{F}_M(q_1^2) \tilde{F}_M(q_2^2) F^{(\text{IP} \text{IP} f_2)}(p_{34}^2) = i\Gamma_{\mu\nu, \kappa\lambda, \rho\sigma}^{(\text{IP} \text{IP} f_2)(1)} \frac{1}{1 - t_1/\tilde{\Lambda}_0^2} \frac{1}{1 - t_2/\tilde{\Lambda}_0^2} \frac{\Lambda_{f_2, P}^4}{\Lambda_{f_2, P}^4 + (p_{34}^2 - m_{f_2}^2)^2}. \quad (5)$$

The $g_{\text{IP} \text{IP} f_2}^{(1)}$ coupling constant and form-factor cutoff parameters $\tilde{\Lambda}_0$, $\Lambda_{f_2, P}$ are treated as free parameters which could be adjusted to fit the experimental data. We take a simple Breit-Wigner form for the $f_2(1950)$ propagator. The $f_2 K^* \bar{K}^*$ vertex is as follows ($M_0 \equiv 1 \text{ GeV}$):

$$i\Gamma_{\mu\nu\kappa\lambda}^{(f_2 K^* \bar{K}^*)}(p_3, p_4) = i \frac{2}{M_0^3} g_{f_2 K^* \bar{K}^*}^{(1)} \Gamma_{\mu\nu\kappa\lambda}^{(0)}(p_3, p_4) F^{(f_2 K^* \bar{K}^*)}(p_{34}^2) - i \frac{1}{M_0} g_{f_2 K^* \bar{K}^*}^{(2)} \Gamma_{\mu\nu\kappa\lambda}^{(2)}(p_3, p_4) F^{(f_2 K^* \bar{K}^*)}(p_{34}^2) \quad (6)$$

with two rank-four tensor functions (see Eqs. (3.18) and (3.19) of [2]). We assume $F^{(f_2 K^* \bar{K}^*)}(p_{34}^2) = F^{(f_2 K^* \bar{K}^*)}(p_{34}^2) = F^{(\text{IP} \text{IP} f_2)}(p_{34}^2)$ and $\Lambda_{f_2}^{(1)} = \Lambda_{f_2}^{(2)} = \Lambda_{f_2, P}$. Thus, the result will depend on the product of the couplings $g_{\text{IP} \text{IP} f_2}^{(1)} g_{f_2 K^* \bar{K}^*}^{(1)}$ and $g_{\text{IP} \text{IP} f_2}^{(1)} g_{f_2 K^* \bar{K}^*}^{(2)}$. In the following we assume that only either the first or the second of the product of couplings is nonzero.

Continuum mechanism: We take into account the reggeization of intermediate \hat{t} -, \hat{u} -channel K^* meson. The $\text{IP} K^* K^*$ vertex, with k', μ and k, ν the momentum and vector index of the outgoing and incoming K^* , respectively, and $\kappa\lambda$ the tensor IP indices, reads

$$i\Gamma_{\mu\nu\kappa\lambda}^{(\text{IP} K^* K^*)}(k', k) = i \left[2a_{\text{IP} K^* K^*} \Gamma_{\mu\nu\kappa\lambda}^{(0)}(k', -k) - b_{\text{IP} K^* K^*} \Gamma_{\mu\nu\kappa\lambda}^{(2)}(k', -k) \right] \frac{1}{1 - (k' - k)^2/\Lambda_0^2} \hat{F}_{K^*}(\hat{p}^2). \quad (7)$$

Here, the form factors $\hat{F}_{K^*}(\hat{p}_t^2)$ and $\hat{F}_{K^*}(\hat{p}_u^2)$ are parametrised in the exponential form. We assume that $a \neq 0$, $b = 0$ or $a = 0$, $b \neq 0$. The coupling and cutoff parameters ($a_{\text{IP} K^* K^*}$, $b_{\text{IP} K^* K^*}$, Λ_0 , $\Lambda_{\text{off}, E}$) could be adjusted to experimental data.

Comparison with the WA102 data at $\sqrt{s} = 29.1$ GeV and predictions for the LHC experiments

In our exploratory study we consider separately the two mechanisms shown by the diagrams in Fig. 1.

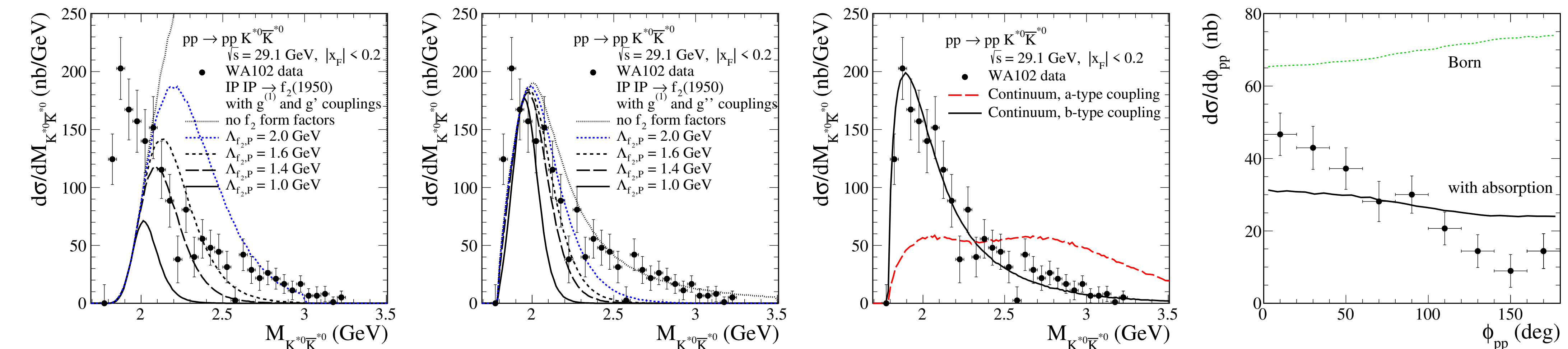


Fig.2: The distributions in $K^{*0}\bar{K}^{*0}$ invariant mass for the $f_2(1950)$ mechanism (two first panels) and for the continuum mechanism (third panel) compared to the WA102 data ($\sigma_{\text{exp}} = 85 \pm 10$ nb [4]). The model results, in both cases, are in better agreement with the WA102 data for the tensor-vector-vector coupling vertices $\propto \Gamma^{(2)}$. The absorption effects were included. Absorption leads to a reduction of the cross section and change the shape of the ϕ_{pp} distribution, the azimuthal angle between the transverse momentum vectors of the outgoing protons.

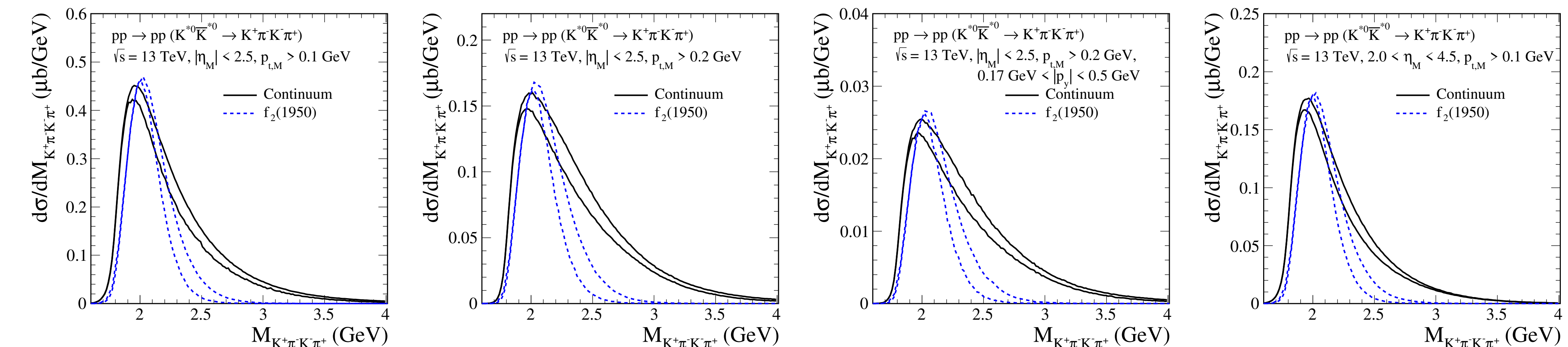


Fig.3: Invariant mass distributions for the $K^+K^-\pi^+\pi^-$ system calculated for $\sqrt{s} = 13$ TeV and for typical experimental cuts on pseudorapidities and transverse momenta of produced pions and kaons. We show the results with an extra cut on momenta of outgoing protons that will be measured in the ATLAS+ALFA experiment and the results for larger η_M and without a measurement of protons relevant for the LHCb experiment. For the $f_2(1950)$ contribution the results for $\Lambda_{f_2, P} = 1.6$ GeV (lower blue line) and 2 GeV (upper blue line) are presented. For the continuum term we show the results for two parametrisations of the K^* Regge trajectory: the linear form (lower black line) and the nonlinear (square-root) form from *M. Brisudova et al., PRD 61 (2000) 054013* (upper black line). The absorption effects were included in the calculations.

Conclusions

- We have discussed in detail the reaction $pp \rightarrow ppK^{*0}\bar{K}^{*0}$ through two different diffractive mechanisms within the tensor-pomeron approach [2]: CEP of the $f_2(1950)$ resonance and the continuum with the intermediate K^{*0} -meson exchange; for more details see [1]. We obtain a good description of the WA102 data [4] assuming that the reaction is dominated by pomeron exchange already at $\sqrt{s} = 29.1$ GeV. Therefore, our predictions for the LHC experiments should be regarded rather as an upper limit. We find that including the continuum contribution alone one can describe the WA102 data reasonably well (see the third and fourth panels of Fig.2).
- We have presented predictions for the reaction $pp \rightarrow ppK^+K^-\pi^+\pi^-$ for the LHC experiments at $\sqrt{s} = 13$ TeV. We obtain from our model $\sigma \simeq 17 - 250$ nb, depending on the assumed cuts. Both considered mechanisms have a maximum around $M_{2K2\pi} \simeq 2$ GeV, thus a broad enhancement (at least part of it) in this mass region can be misidentified as the $f_2(1950)$ resonance (one of the candidates for tensor-gluon state). A similar behaviour of these mechanisms makes an identification of a tensor-gluon state in this reaction rather difficult. Their theoretical calculation is a challenging problem of nonperturbative QCD.

[1] P. Lebedowicz, Phys. Rev. D103 (2021) 054039; [2] C. Ewerz, M. Maniatis, O. Nachtmann, Annals Phys. 342 (2014) 31;

[3] P. Lebedowicz, O. Nachtmann, A. Szczurek, Phys. Rev. D93 (2016) 054015; see also Phys. Rev. D101 (2020) 034008;

[4] D. Barberis et al., (WA102 Collaboration), Phys. Lett. B436 (1998) 204